arXiv:nucl-th/0312060v1 16 Dec 2003

Iterated and irreducible pion-photon exchange in nuclei

N. Kaiser

Physik Department T39, Technische Universität München, D-85747 Garching, Germany

Abstract

We calculate the contribution to the nuclear energy density functional which arises from iterated pion-photon exchange between nucleons. In heavy nuclei, this novel charge symmetry breaking interaction leads to an additional binding of each proton by about 0.2 MeV. Compared to that the analogous effect from irreducible pion-photon exchange is negligibly small. As a possible mechanism to resolve the Nolen-Schiffer anomaly we propose the iteration of one-photon exchange with an attractive short-range NN-interaction. The corresponding energy per proton reads: $\bar{E}[\rho_p] = (2\alpha/15\pi^2)(\pi^2 - 3 + 6\ln 2)\mathcal{A}_{pp}\, k_p^2$ with $\rho_p = k_p^3/3\pi^2$ the proton density and $\mathcal{A}_{pp} \approx 2\,\mathrm{fm}$ an effective (in-medium) scattering length. Hints for such a value of $\mathcal{A}_{pp}$ come from phenomenological Skyrme forces and from the neutron matter equation of state.

PACS: 12.38.Bx, 21.10.Sf, 31.15.Ew.

A classic problem in nuclear structure theory is to understand the binding energy differences between mirror nuclei (i.e. nuclei with the same mass number $A = Z + N$ but with the proton number Z and the neutron number N interchanged). If the strong nuclear force is charge symmetric, then these binding energy differences can be directly related to the well-understood Coulomb interaction between the protons. However, as shown long ago by Nolen and Schiffer [1, 2] the experimental binding energy differences are systematically (by about 7%) larger than the ones calculated with a charge symmetric strong interaction and realistic nuclear wave functions (reproducing e.g. elastic electron-scattering data). This discrepancy which ranges from fairly light up to the heaviest available mirror nuclei is called the Nolen-Schiffer anomaly. It is generally agreed that both nuclear correlations [3] and a charge-symmetry breaking strong interaction are important for its understanding.

Recently, Brown et al. [4] have performed a systematic study of these binding energy differences the mass region $A \leq 60$ using the Skyrme-Hartree-Fock method. They have found that the anomaly can be resolved by either dropping the (weakly) attractive Coulomb exchange term in the nuclear energy density functional (see eqs.(5,7) below) or by introducing a charge-symmetry breaking delta-force which splits the proton-proton and neutron-neutron effective s-wave interactions. The strength of the adjusted charge-symmetry breaking interaction comes out, however, a factor 3 to 4 larger than expected from some high-precision nucleon-nucleon potentials (such as AV18 [5] or CDBonn [6]). Henley and Krein [7] suggested an alternative explanation of the Nolen-Schiffer anomaly based on the quark substructure of nucleons in the nuclear medium. In their Nambu-Jona-Lasinio model the down-up-quark mass difference induces, driven by the partial restoration of chiral symmetry, a substantial reduction of the neutron-proton mass difference in the nuclear medium (see Fig. 2b in ref.[7]). Clearly, any decrease of the neutron-proton mass difference will help to resolve the Nolen-Schiffer anomaly, since the calculated binding energy differences of mirror nuclei are based on the free neutron-proton mass difference of 1.293 MeV. For a similar approach using the quark-meson coupling

model, see ref.[8]. In this context it should also be noted that most relativistic (scalar-vector) mean-field models for nuclear structure leave out the (attractive) Coulomb exchange term by default and thus circumvent the problem.

In this work we will use chiral perturbation theory to calculate the leading order long-range charge-symmetry breaking effects generated by the combined pion- and photon-exchange between nucleons. We present analytical results for the corresponding contributions to the nuclear energy density functional. This energy density functional actually defines a general starting point for (non-relativistic) nuclear structure calculations within the self-consistent mean-field approximation [9]. It turns out that the three-loop in-medium diagrams of iterated pion-photon exchange and of irreducible pion-photon exchange contribute at different orders in the small momentum expansion. This allows us even to draw some conclusions about convergence properties.

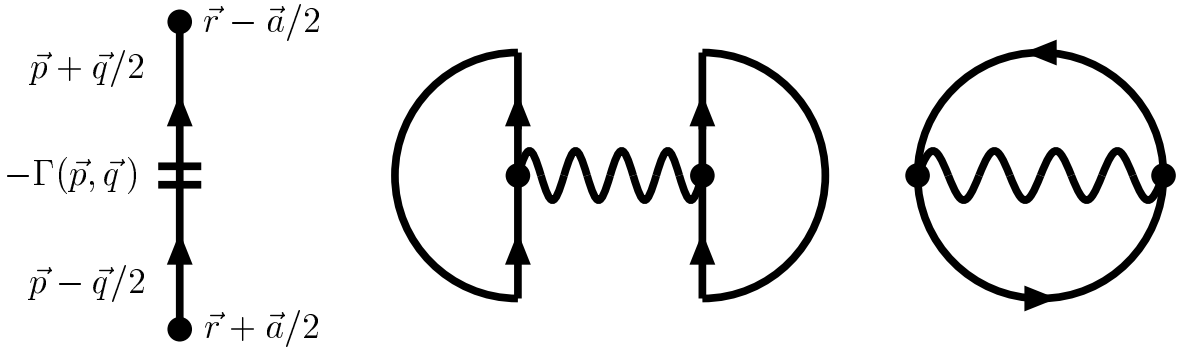

Fig. 1: Left: The double line symbolizes the medium insertion $\Gamma(\vec{p},\vec{q})$ defined by eq.(4). Next shown are the two-loop one-photon exchange Hartree and Fock diagrams. Their combinatoric factor is 1/2.

The starting point for the construction of an explicit nuclear energy density functional is the density-matrix as given by a sum over the occupied energy eigenfunctions Ψ_ν. We restrict here the formulation to the proton-states since only these participate in the Coulomb interaction. According to Negele and Vautherin [10] the bilocal density-matrix can be expanded in relative and center-of-mass coordinates, $\vec{a}$ and $\vec{r}$, as follows:

$$\sum_{\nu\in\mathrm{occ}} \Psi_\nu(\vec{r}-\vec{a}/2)\Psi_\nu^\dagger(\vec{r}+\vec{a}/2) \;=\; \frac{3\rho_p}{ak_p}\,j_1(ak_p) - \frac{35}{2ak_p^3}\,j_3(ak_p)\Big[\tau_p - \frac{3}{5}\rho_p k_p^2 - \frac{1}{4}\vec{\nabla}^2\rho_p\Big]\,, \quad (1)$$

where $j_{1,3}(ak_p)$ are ordinary spherical Bessel functions. The other quantities on the right hand side of eq.(1) are the local proton density:

$$\rho_p(\vec{r}) = \frac{k_p^3(\vec{r})}{3\pi^2} = \sum_{\nu\in\mathrm{occ}} \Psi_\nu^\dagger(\vec{r})\Psi_\nu(\vec{r})\,, \quad (2)$$

written in terms of a local proton Fermi-momentum $k_p(\vec{r})$, and the local proton kinetic energy density:

$$\tau_p(\vec{r}) = \sum_{\nu\in\mathrm{occ}} \vec{\nabla}\Psi_\nu^\dagger(\vec{r})\cdot\vec{\nabla}\Psi_\nu(\vec{r})\,. \quad (3)$$

The Fourier transform of the expanded density-matrix in eq.(1) with respect to both coordinates $\vec{a}$ and $\vec{r}$ defines a "medium insertion" for the inhomogeneous many-fermion system

[11]:

$$\Gamma(\vec{p},\vec{q}\,) = \int d^3r\, e^{-i\vec{q}\cdot\vec{r}}\,\theta(k_p-|\vec{p}\,|)\left\{1+\frac{35\pi^2}{4k_p^7}(5\vec{p}^{\,2}-3k_p^2)\Big[\tau_p-\frac{3}{5}\rho_p k_p^2-\frac{1}{4}\vec{\nabla}^2\rho_p\Big]\right\}. \qquad (4)$$

The double line in Fig. 1 symbolizes this medium insertion together with the assignment of the out- and in-going momenta $\vec{p}\pm\vec{q}/2$. The momentum transfer $\vec{q}$ is provided by the Fourier components of the inhomogeneous (proton) distributions $\rho_p(\vec{r}\,)$ and $\tau_p(\vec{r}\,)$. Going up to second order in spatial gradients (i.e. deviations from homogeneity) the protonic energy density functional reads:

$$\mathcal{E}[\rho_p,\tau_p] = \rho_p\bar{E}[\rho_p] + \Big[\tau_p-\frac{3}{5}\rho_p k_p^2-\frac{1}{4}\vec{\nabla}^2\rho_p\Big]F_\tau(\rho_p)\,. \qquad (5)$$

Here, the functional $\bar{E}[\rho_p]$ denotes the energy per proton. The other strength function $F_\tau(\rho_p)$ is related to the effective proton mass by the relation: $\widetilde{M}^*(\rho_p) = M[1+2MF_\tau(\rho_p)]^{-1}$, where $M = 938.272\,\mathrm{MeV}$ denotes the free proton mass. We apply the density-matrix formalism first to the one-photon exchange diagrams in Fig. 1. From the Hartree diagram one regains the well-known classical result:

$$\bar{E}[\rho_p] = \frac{\alpha}{2}\int d^3r'\frac{\rho_p(\vec{r}\,')}{|\vec{r}-\vec{r}\,'|} = \frac{2\pi\alpha}{r}\int_0^\infty dr' r'\rho_p(r')\mathrm{min}(r,r')\,, \qquad (6)$$

with $\alpha = 1/137.036$ the fine structure constant. The simplification of expression for the Coulomb potential in the second part of eq.(6) holds for a spherically symmetric proton density $\rho_p(r')$. The result of the one-photon exchange Fock diagram is also well-known [12]:

$$\bar{E}[\rho_p] = -\frac{3\alpha}{4\pi}\,k_p\,, \qquad\qquad F_\tau(\rho_p) = \frac{35\alpha}{36\pi k_p}\,. \qquad (7)$$

The derivative of the corresponding energy density with respect to the proton density: $\partial(\rho_p\bar{E}[\rho_p])/\partial\rho_p = -\alpha k_p/\pi$, is sometimes also referred to as the Coulomb exchange term [4].

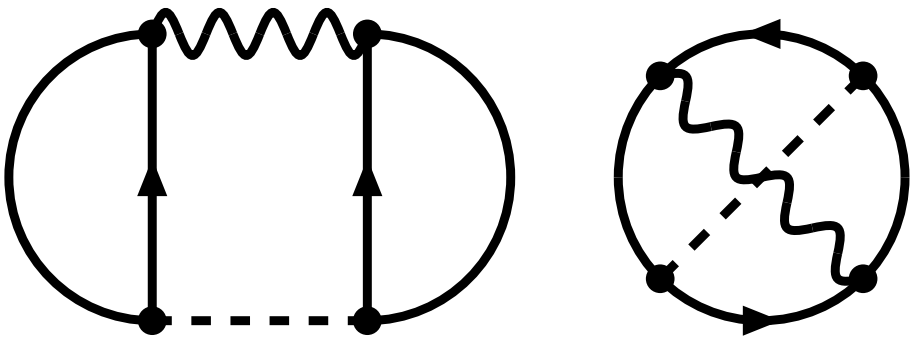

Fig. 2: Iterated pion-photon exchange Hartree and Fock diagrams. Their combinatoric factor is 1/2.

Next, we consider pion-loop corrections to the one-photon exchange diagrams in Fig. 1. There are many possible diagrams, some introduce vacuum polarization, others generate (contributions to) the proton electric form factor and another class builds up the $\pi\gamma$-exchange nucleon-nucleon potential (see eq.(16) below). The two diagrams of iterated pion-photon exchange shown in Fig. 2 are however special and distinguished by the feature of carrying an

energy denominator equal to the difference of nucleon kinetic energies. These two diagrams get enhanced by the large scale factor M and therefore they are expected to be dominant. The left Hartree diagram in Fig. 2 is easily seen to vanish as a consequence of a zero spin-trace, $\mathrm{tr}(\vec{\sigma}\cdot\vec{l})=0$. The evaluation of the iterated $\pi\gamma$-exchange Fock diagram with two medium insertions (on non-neighboring nucleon propagators) leads to the loop integral:

$$\int\!\!\!\!\!\!-\frac{d^3l}{2\pi^2}\frac{(\vec{l}+\vec{Q})^2}{[m_\gamma^2+\vec{l}^{\,2}]\,[m_\pi^2+(\vec{l}+\vec{Q})^2]\,\vec{l}\cdot(\vec{l}+\vec{Q})}=\frac{1}{Q(m_\pi^2+m_\gamma^2+Q^2)}$$
$$\times\left[(m_\gamma^2+Q^2)\arctan\frac{Q}{m_\gamma}-m_\pi^2\arctan\frac{Q}{m_\pi}+2m_\pi^2\arctan\frac{Q}{m_\pi+m_\gamma}\right], \qquad (8)$$

which has been regularized by introducing an infinitesimal photon mass m_γ. Taking the limit $m_\gamma\to 0$ of the analytical expression in eq.(8) one gets the following infrared-finite result for the loop integral:

$$\frac{1}{m_\pi^2+Q^2}\left[\frac{\pi}{2}|Q|+\frac{m_\pi^2}{Q}\arctan\frac{Q}{m_\pi}\right]. \qquad (9)$$

We warn that by setting $m_\gamma=0$ in the loop integrand and performing some seemingly harmless manipulations one can arrive at an incorrect result which misses the $\pi|Q|/2$ term in eq.(9). After further reduction of the integral over the product of two Fermi spheres of radius k_p one obtains the following contribution to the energy per proton:

$$\bar{E}[\rho_p]=-\frac{\alpha g_{\pi N}^2 m_\pi^2}{4\pi^2 M u^3}\int_0^u dx\,x(u-x)^2(2u+x)\frac{2\pi x^2+\arctan 2x}{1+4x^2}\,, \qquad (10)$$

with the abbreviation $u=k_p/m_\pi$. We choose the value $g_{\pi N}=13.2$ for the pion-nucleon coupling constant and $m_\pi=135\,\mathrm{MeV}$ stands for the neutral pion mass. In order to recover the enhancement factor M in eq.(10) one has to remember that the pseudovector πNN-vertex carries the prefactor $g_{\pi N}/2M$. The contribution to the strength function $F_\tau(\rho_p)$ reads:

$$F_\tau(\rho_p)=\frac{35\alpha g_{\pi N}^2}{12\pi^2 M u^7}\int_0^u dx\,x^2(u-x)^2(3u^2-4ux-2x^2)\frac{2\pi x^2+\arctan 2x}{1+4x^2}\,, \qquad (11)$$

where we have made use of the master integral eq.(A1) in ref.[11]. An in-medium diagram with three medium insertions represents Pauli-blocking effects. We obtain from the iterated $\pi\gamma$-exchange Fock diagram with three medium insertions the following contributions to the energy per proton:

$$\bar{E}[\rho_p]=\frac{3\alpha g_{\pi N}^2 m_\pi^2}{16\pi^3 M u^3}\int_0^u dx\,x^2\int_{-1}^1 dy\int_{-1}^1 dz\,\frac{yz\,\theta(y^2+z^2-1)}{|yz|\sqrt{y^2+z^2-1}}\Big[s^2-\ln(1+s^2)\Big]\ln t\,, \qquad (12)$$

and to the strength function $F_\tau(\rho_p)$:

$$F_\tau(\rho_p) = \frac{175\alpha g_{\pi N}^2}{64\pi^3 M u^7}\int_0^u dx\,x^2\int_{-1}^1 dy\int_{-1}^1 dz\,\frac{yz\,\theta(y^2+z^2-1)}{|yz|\sqrt{y^2+z^2-1}}\Bigg\{\Big[\ln(1+s^2)-s^2\Big]$$
$$\times\left[txz+\left(\frac{9}{5}u^2+1-3x^2\right)\ln t\right]+\left[4xy\left(s-\frac{s^3}{3}-\arctan s\right)+\frac{s^4}{2}\right]\ln t\Bigg\}. \qquad (13)$$

Here, $s=xy+\sqrt{u^2-x^2+x^2y^2}$ and $t=xz+\sqrt{u^2-x^2+x^2z^2}$ are auxiliary functions which emerge in the reduction [11] of a nine-dimensional principal value integral over the product

of three Fermi spheres of radius k_p. The infrared finiteness of the results eqs.(12,13) deserves some closer inspection. In the actual calculation the logarithmic term $\ln t$ is accompanied by an additive constant $\ln(m_\pi/m_\gamma)$. However, when integrated over z the infrared-singular constant $\ln(m_\pi/m_\gamma)$ drops out since the integrand is odd under the substitution $z \to -z$. It is also interesting to consider the chiral limit of vanishing pion mass $m_\pi = 0$. In that case all integrals occurring in eqs.(10-13) can be solved in closed form. One finds a simple $\rho_p^{2/3}$-behavior of the energy per proton:

$$\bar{E}[\rho_p]\Big|_{m_\pi=0} = \frac{\alpha g_{\pi N}^2 k_p^2}{120\pi^3 M}\Big(3 - \pi^2 - 6\ln 2\Big) \simeq -1.50\,\mathrm{MeVfm}^2 \cdot \rho_p^{2/3}\,, \tag{14}$$

and a density independent strength function $F_\tau(\rho_p)$:

$$F_\tau(\rho_p)\Big|_{m_\pi=0} = \frac{\alpha g_{\pi N}^2}{\pi^3 M}\Big(\frac{13}{64} - \frac{2}{3}\ln 2\Big) \simeq -0.441\,\mathrm{MeVfm}^2\,. \tag{15}$$

While these density dependences could also be guessed through mass dimension counting, the numerical coefficients are highly non-trivial.

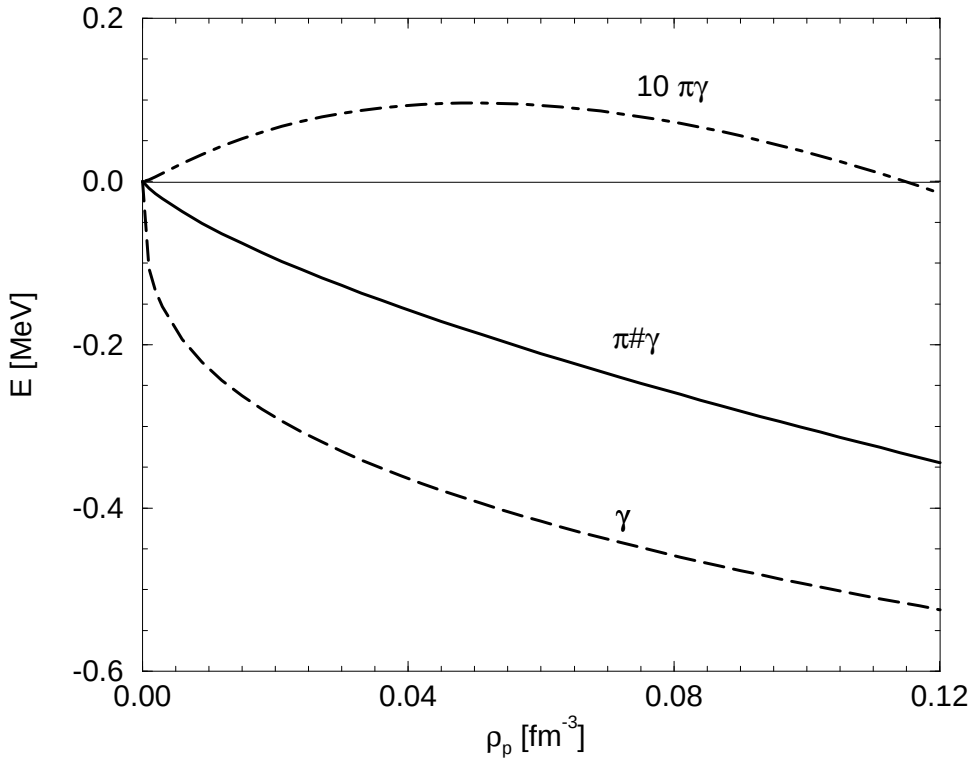

Fig. 3: The energy per proton $\bar{E}[\rho_p]$ versus the proton density $\rho_p = k_p^3/3\pi^2$. The dashed and full line show the result of the 1γ-exchange and the iterated $\pi\gamma$-exchange Fock diagram. The dashed-dotted line shows the result of irreducible $\pi\gamma$-exchange, magnified by a factor 10.

In Fig. 3 we show the energy per proton $\bar{E}[\rho_p]$ as a function of the proton density $\rho_p = k_p^3/3\pi^2$. The dashed line shows the result $\bar{E}[\rho_p] = -3\alpha k_p/4\pi$ of the one-photon exchange Fock diagram. The full line gives the result of the iterated pion-photon exchange Fock diagram (evaluated with a finite pion mass of $m_\pi = 135\,\mathrm{MeV}$). One notices that both energy densities

lead in nuclei to an attraction between the protons. Furthermore, as it should be for a higher order correction, iterated $\pi\gamma$-exchange comes out a factor of about two smaller than 1γ-exchange. The density dependence of the full line in Fig. 3 is well approximated by the fit function: $\bar{E}[\rho_p]^{\pi\gamma} \simeq -1.4\,\mathrm{MeVfm}^2 \cdot \rho_p^{2/3}$. Interestingly, it does not differ much from the result eq.(14) valid in the strict chiral limit $m_\pi = 0$.

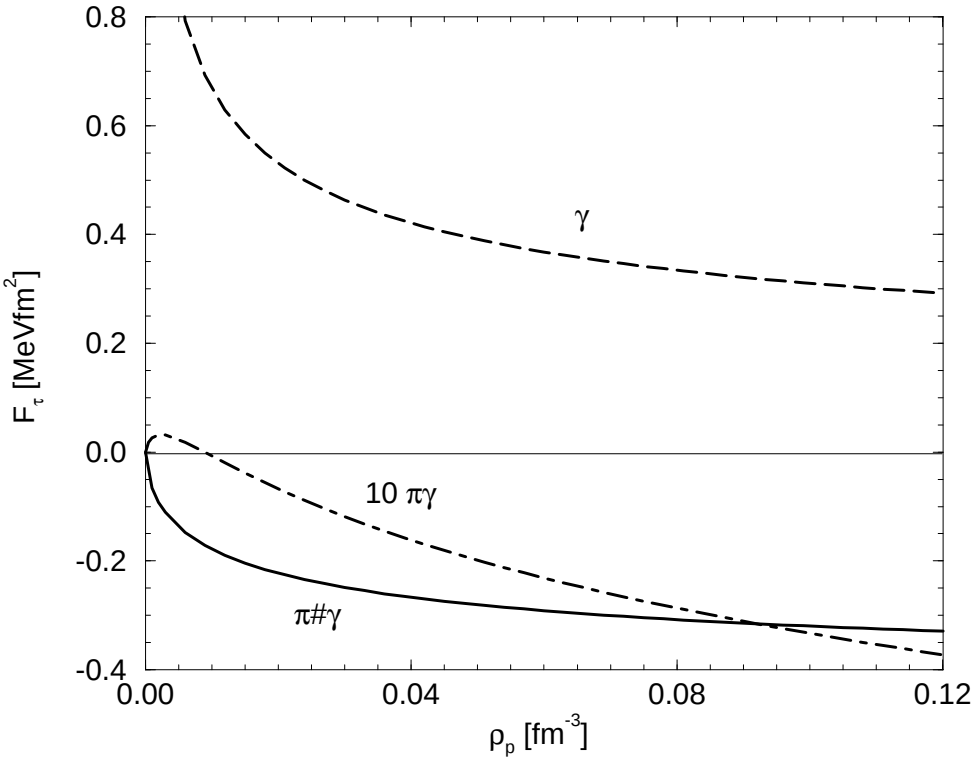

Fig. 4: The strength function $F_\tau(\rho_p)$ versus the proton density $\rho_p = k_p^3/3\pi^2$. The dashed and full line show the result of the 1γ-exchange and the iterated $\pi\gamma$-exchange Fock diagram. The dashed-dotted line shows the result of irreducible $\pi\gamma$-exchange, magnified by a factor 10.

In Fig. 4 we show the strength function $F_\tau(\rho_p)$ versus the proton density $\rho_p = k_p^3/3\pi^2$. The dashed line shows the result $F_\tau(\rho_p) = 35\alpha/36\pi k_p$ of the one-photon exchange Fock diagram and the full line gives the result of the iterated pion-photon exchange Fock diagram. One observes a strong cancelation between both contributions, in particular at higher proton densities $\rho_p > 0.06\,\mathrm{fm}^{-3}$. Therefore one may neglect with good reason the part of the energy density functional proportional to $F_\tau(\rho_p)$ in nuclear structure calculations.

For a numerical estimate of the Coulomb energies of nuclei we choose radially symmetric proton densities of Saxon-Woods type: $\rho_p(r) \sim [1 + \exp((r-R)/a)]^{-1}$, with a diffuseness parameter of $a = 0.54\,\mathrm{fm}$ and a mean nuclear radius of $R = 1.07\,\mathrm{fm}\cdot A^{1/3}$ (where A is the mass number). The proton density $\rho_p(r)$ of a given nucleus is normalized to its total proton number $Z = 4\pi \int_0^\infty dr r^2 \rho_p(r)$ and the Coulomb energy is then calculated via: $E_{\mathrm{Coul}} = 4\pi \int_0^\infty dr r^2 \rho_p(r) \bar{E}[\rho_p(r)]$. In Tab. 1 we list numerical values of the Coulomb energies per proton E_{Coul}/Z for a few selected nuclei: Ca, Fe, Sn and Pb. The direct Coulomb term (labeled 1γ-Hartree) gives of course the dominant repulsive contribution which increases with the proton number Z. The Coulomb exchange term (labeled 1γ-Fock) is weakly attractive and almost independent of the proton number Z. The same features hold for the iterated

$\pi\gamma$-exchange Fock diagram which gives numerical values of $E_{\rm Coul}/Z$ about half as large as those of the Coulomb exchange term. One can infer from Tab. 1 that iterated $\pi\gamma$-exchange leads to an additional binding of each proton in a heavy nucleus by about 0.2 MeV. This unique long-range charge-symmetry breaking interaction does therefore not help to resolve the Nolen-Schiffer anomaly. On the contrary, it even further enhances the discrepancies.

$E_{\rm Coul}/Z$ [MeV]	Ca	Fe	Sn	Pb
1γ-Hartree	3.94	4.72	7.44	10.43
1γ-Fock	–0.37	–0.37	–0.38	–0.39
$\pi\gamma$-Fock	–0.18	–0.18	–0.19	–0.20

Tab.1: Numerical values of Coulomb energies per proton for various nuclei. The units of $E_{\rm Coul}/Z$ are MeV.

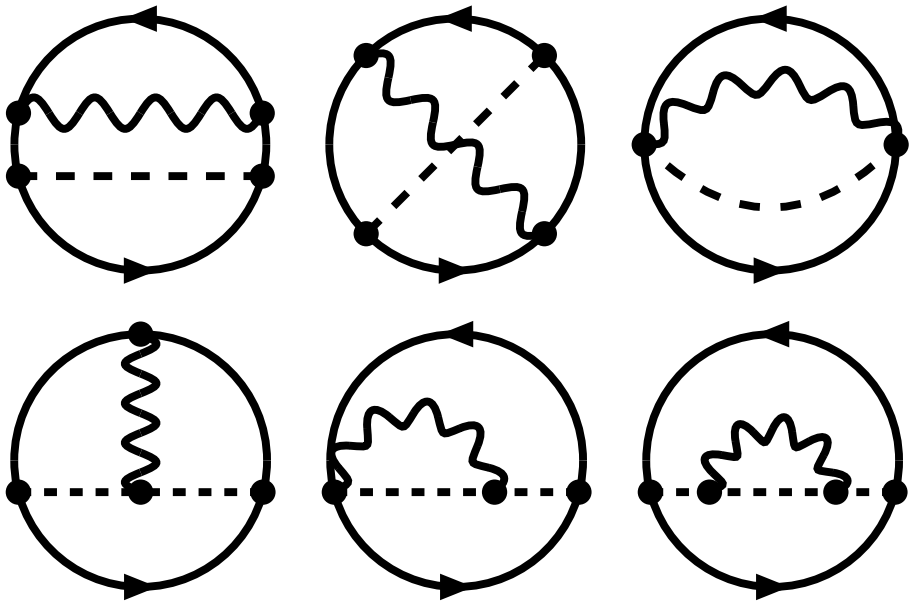

Fig. 5: Fock diagrams of irreducible pion-photon exchange. Their combinatoric factors are 1, 1/2, 1/2, 1, 1 and 1/2, in the order shown.

Next, we consider irreducible pion-photon exchange which is of subleading order in the small momentum expansion (no large scale enhancement factor M is present). The relevant set of Fock diagrams contributing to the energy density functional is shown in Fig. 5. The corresponding Hartree diagrams (with two closed nucleon lines) vanish again due to a zero spin-trace. By opening two nucleon lines of the diagrams in Fig. 5 one encounters the NN-scattering T-matrix related to irreducible $\pi\gamma$-exchange between nucleons. This T-matrix has recently been calculated in chiral perturbation theory by van Kolck et al. [13]. We reproduce independently their analytical result:

$$T_{\pi\gamma}(\vec{Q}) = \frac{\alpha g_{\pi N}^2}{8\pi M^2}(\vec{\tau}_1\cdot\vec{\tau}_2 - \tau_1^3\tau_2^3)\,\vec{\sigma}_1\cdot\vec{Q}\,\vec{\sigma}_2\cdot\vec{Q}\left\{\frac{1}{Q^2} - \frac{(m_\pi^2-Q^2)^2}{Q^4(m_\pi^2+Q^2)}\ln\left(1+\frac{Q^2}{m_\pi^2}\right)\right\}. \qquad (16)$$

Here, $\vec{\sigma}_{1,2}$ and $\vec{\tau}_{1,2}$ denote the spin- and isospin-operators of the two nucleons and $\vec{Q}$ is the momentum transfer between both nucleons. Obviously, the charge-symmetry breaking T-matrix in eq.(16) can only contribute to elastic $pn \to np$ scattering. The corresponding energy density depends therefore on the product of the proton and the neutron density. For the sake of simplicity we assume these densities to be equal and obtain then the following contributions from irreducible $\pi\gamma$-exchange to the energy per proton:

$$\bar{E}[\rho_p] = \frac{\alpha g_{\pi N}^2 m_\pi^3}{8\pi^3 M^2}\left\{\frac{u^3}{3} - \int_0^u dx\,\frac{(u-x)^2(2u+x)}{u^3(1+4x^2)}(1-4x^2)^2\ln(1+4x^2)\right\}, \tag{17}$$

and to the strength function $F_\tau(\rho_p)$:

$$F_\tau(\rho_p) = \frac{35\alpha g_{\pi N}^2 m_\pi}{24\pi^3 M^2 u^7}\int_0^u dx\, x(u-x)^2(3u^2-4ux-2x^2)\frac{(1-4x^2)^2}{1+4x^2}\ln(1+4x^2)\,. \tag{18}$$

The density dependence of these results (magnified by a factor of 10) is shown by the dashed-dotted lines in Figs. 3,4. One observes that the contributions from irreducible $\pi\gamma$-exchange are negligibly small. The Coulomb energies per proton $E_{\rm Coul}/Z$ are affected at the level of a few keV. Such tiny repulsive corrections can of course not help to resolve the Nolen-Schiffer anomaly. For the sake of completeness we consider also the behavior of the expressions in eqs.(17,18) in the chiral limit, $m_\pi \to 0$, and find:

$$\bar{E}[\rho_p]\Big|_{m_\pi\to 0} = \frac{\alpha g_{\pi N}^2 k_p^3}{12\pi^3 M^2}\Big(\frac{5}{4} - \ln\frac{2k_p}{m_\pi}\Big)\,, \qquad F_\tau(\rho_p)\Big|_{m_\pi=0} = -\frac{7\alpha g_{\pi N}^2 k_p}{96\pi^3 M^2}\,. \tag{19}$$

In order to resolve the Nolen-Schiffer anomaly a dynamical mechanism is needed which generates additional repulsion for the protons but leaves the neutrons unaffected. Inspired by eq.(14), we propose as such a possible mechanism the iteration of a short-range attractive NN-interaction with the (repulsive) one-photon exchange. For its explicit evaluation consider the three-loop diagrams in Fig. 2 with the dashed line symbolizing now a heavy scalar meson. The ratio g_s/m_s of the scalar meson's coupling constant and mass merely serves to introduce an effective scattering length $\mathcal{A}_{pp} = (g_s/m_s)^2 M/4\pi$. After performing all occurring integrals we obtain from the iteration of a short-range pp-interaction with one-photon exchange the following contributions to the energy per proton:

$$\bar{E}[\rho_p] = \frac{2\alpha}{15\pi^2}(\pi^2 - 3 + 6\ln 2)\mathcal{A}_{pp}\,k_p^2 \simeq 2.053\,\text{MeVfm}\cdot\mathcal{A}_{pp}\,\rho_p^{2/3}\,, \tag{20}$$

and to the strength function $F_\tau(\rho_p)$:

$$F_\tau(\rho_p) = \frac{\alpha}{\pi^2}\Big(\frac{32}{3}\ln 2 - \frac{13}{4}\Big)\mathcal{A}_{pp}\,. \tag{21}$$

The sign-convention is chosen here such that a positive scattering length $\mathcal{A}_{pp} > 0$ corresponds to attraction.

In order to compensate both the 1γ-exchange Fock contribution and the $\pi\gamma$-exchange Fock contribution an effective pp-scattering length of $\mathcal{A}_{pp} \approx 2\,\text{fm}$ is required. This numerical estimate stems from the numbers in the second and third row of Tab. 1 in combination with eq.(20) and the fit function $\bar{E}[\rho_p]^{\pi\gamma} \simeq -1.4\,\text{MeVfm}^2\cdot\rho_p^{2/3}$. Note that this estimated value of the effective pp-scattering length $\mathcal{A}_{pp} \approx 2\,\text{fm}$ is an order of magnitude smaller than the

free ${}^1S_0$ NN-scattering length $a({}^1S_0) \simeq 19\,\mathrm{fm}$ [14] and therefore it subsumes lots of many-body dynamics being active at finite density. Most interestingly, phenomenological Skyrme forces give a strong indication for such a value of the effective *pp*-scattering length. As a matter of fact, the Skyrme force parameters t_0 and x_0 [4, 9] encode an effective *pp*-scattering length via the relation $\mathcal{A}_{pp} = Mt_0(x_0 - 1)/4\pi$. Inserting the values in Tab. 1 of ref.[15] one finds $\mathcal{A}_{pp} = 1.96\,\mathrm{fm}$, 2.40 fm and 1.83 fm for the forces SKXce, SKXm and SKX, respectively. Averaging over the variants MSk1-6 of ref.[16] one gets for comparison $\mathcal{A}_{pp} = 1.66\,\mathrm{fm}$. A further hint on $\mathcal{A}_{pp}$ comes from the equation of state of pure neutron matter. The result of the sophisticated many-body calculation of the Urbana group [17] is well approximated for neutron densities $\rho_n \leq 0.4\,\mathrm{fm}^{-3}$ by a fourth order polynomial in the neutron Fermi momentum k_n, namely: $\bar{E}_n(k_n) = 3k_n^2/10M - \alpha_n k_n^3/M^2 + \beta_n k_n^4/M^3$, with adjusted coefficients $\alpha_n = 1.247$ and $\beta_n = 2.168$. The coefficient α_n of the term linear in the neutron density $\rho_n = k_n^3/3\pi^2$ can be translated into an effective *nn*-scattering length of $\mathcal{A}_{nn} = 3\pi\alpha_n/M \simeq 2.47\,\mathrm{fm}$ and isospin symmetry implies $\mathcal{A}_{pp} = \mathcal{A}_{nn} \simeq 2.47\,\mathrm{fm}$. Admittedly, these arguments for $\mathcal{A}_{pp} \approx 2\,\mathrm{fm}$ leave some loose ends but there seem to be several interesting cross relations.

In summary, we have calculated in this work the contributions of iterated and irreducible pion-photon exchange to the nuclear energy density functional. These novel terms represent unique long-range charge-symmetry breaking interactions. In heavy nuclei, iterated $\pi\gamma$-exchange leads to an additional binding of each proton by about 0.2 MeV. As a consequence of that the discrepancies between calculated and experimental binding energy differences of mirror nuclei will be further enhanced. The subleading effects from irreducible $\pi\gamma$-exchange turn out to be negligibly small. As a possible mechanism to resolve the Nolen-Schiffer anomaly we propose the iteration of a short-range attractive NN-interaction with one-photon exchange. The corresponding energy per proton has the simple analytical form: $\bar{E}[\rho_p] = (2\alpha/15\pi^2)(\pi^2 - 3 + 6\ln 2)\mathcal{A}_{pp}\, k_p^2$. There are various hints from phenomenological Skyrme forces and from the neutron matter equation of state for an effective *pp*-scattering length with a value around $\mathcal{A}_{pp} \approx 2\,\mathrm{fm}$. In a next (more quantitative) step one should perform nuclear structure calculations (e.g. within the Skyrme-Hartree-Fock approach) which include all the charge-symmetry breaking terms derived in this work. The value of the effective scattering length $\mathcal{A}_{pp}$ should be determined in a best fit to the binding energy differences of mirror nuclei, and one should check the relation $\mathcal{A}_{pp} = Mt_0(x_0 - 1)/4\pi$ to the Skyrme force parameters t_0 and x_0. Of course, a more microscopic interpretation/derivation of it would also be desirable.

References

[1] J.A. Nolen and J.P. Schiffer, *Ann. Rev. Nucl. Sci.* **19**, 471 (1969).

[2] S. Shlomo, *Rep. Prog. Phys.* **41**, 957 (1978).

[3] A. Bulgac and V.R. Shaginyan, *Phys. Lett.* **B469**, 1 (1999).

[4] B.A. Brown, W.A. Richter, and R. Lindsay, *Phys. Lett.* **B483**, 49 (2000); and references therein.

[5] R.B. Wiringa, V.G.J. Stoks, and R. Schiavilla, *Phys. Rev.* **C49**, 2950 (1995).

[6] R. Machleidt, *Phys. Rev.* **C63**, 024001 (2001); and references therein.

[7] E.M. Henley and G. Krein, *Phys. Rev. Lett.* **62**, 2586 (1989).

[8] K. Tsushima, K. Saito, and A.W. Thomas, *Phys. Lett.* **B465**, 36 (1999).

[9] M. Bender, P.-H. Heenen, and P.-G. Reinhard, *Rev. Mod. Phys.* **75**, 121 (2003); and references therein.

[10] J.W. Negele and D. Vautherin, *Phys. Rev.* **C5**, 1472 (1972).

[11] N. Kaiser, S. Fritsch, and W. Weise, *Nucl. Phys.* **A724**, 47 (2003).

[12] C. Titin-Schnaider and P. Quentin, *Phys. Lett.* **B49**, 397 (1974).

[13] U. van Kolck, M.C.M. Rentmeester, J.L. Friar, T. Goldman, and J.J. de Swart, *Phys. Rev. Lett.* **80**, 4386 (1998); and references therein.

[14] D.E. Gonzalez Trotter et al., *Phys. Rev. Lett.* **83**, 3788 (1999); and references therein.

[15] B.A. Brown, *Phys. Rev.* **C58**, 220 (1998).

[16] F. Tondour, S. Goriely, J.M. Pearson, and M. Onsi, *Phys. Rev.* **C62**, 024308 (2000).

[17] B. Friedman and V.R. Pandharipande, *Nucl. Phys.* **A361**, 502 (1981).